Aalborg Universitet

AALBORG UNIVERSITY
DENMARK

A Neural-Network-Based Model Predictive Control of Three-Phase Inverter With an Output LC Filter

Mohamed, Ihab S.; Rovetta, Stefano; Do, Ton Duc; Dragicevic, Tomislav; Diab, Ahmed A. Zaki

Link to publication from Aalborg University

A Neural-Network-Based Model Predictive Control of Three-Phase Inverter With an Output *LC* Filter

IHAB S. MOHAMED[ID]1, STEFANO ROVETTA[ID]2, (Senior Member, IEEE),
TON DUC DO[ID]3, (Member, IEEE), TOMISLAV DRAGIČEVIĆ[ID]4, (Senior Member, IEEE),
AND AHMED A. ZAKI DIAB[ID]5

[1]INRIA Sophia Antipolis—Méditerranée, University Côte d'Azur, 06100 Nice, France
[2]Department of Informatics, Bioengineering, Robotics and Systems Engineering, University of Genoa, 16126 Genoa, Italy
[3]Department of Robotics and Mechatronics, School of Engineering and Digital Sciences (SEDS), Nazarbayev University, Z05H0P9 Nur-Sultan, Kazakhstan
[4]Department of Energy Technology, Aalborg University, 9100 Aalborg, Denmark
[5]Electrical Engineering Department, Faculty of Engineering, Minia University, Minya 61111, Egypt

Corresponding author: Ton Duc Do (doduc.ton@nu.edu.kz)

ABSTRACT Model predictive control (MPC) has become one of the well-established modern control methods for three-phase inverters with an output *LC* filter, where a high-quality voltage with low total harmonic distortion (THD) is needed. Although it is an intuitive controller, easy to understand and implement, it has the significant disadvantage of requiring a large number of online calculations for solving the optimization problem. On the other hand, the application of model-free approaches such as those based on artificial neural networks approaches is currently growing rapidly in the area of power electronics and drives. This paper presents a new control scheme for a two-level converter based on combining MPC and feed-forward ANN, with the aim of getting lower THD and improving the steady and dynamic performance of the system for different types of loads. First, MPC is used, as an expert, in the training phase to generate data required for training the proposed neural network. Then, once the neural network is fine-tuned, it can be successfully used online for voltage tracking purpose, without the need of using MPC. The proposed ANN-based control strategy is validated through simulation, using MATLAB/Simulink tools, taking into account different loads conditions. Moreover, the performance of the ANN-based controller is evaluated, on several samples of linear and non-linear loads under various operating conditions, and compared to that of MPC, demonstrating the excellent steady-state and dynamic performance of the proposed ANN-based control strategy.

INDEX TERMS Three-phase inverter, model predictive control, artificial neural network, UPS systems.

I. INTRODUCTION

The three-phase inverter is an extensively popular device, which is commonly used for transferring energy from a DC voltage source to an AC load. The control of three-phase inverters has received much attention in the last decades both in the scientific literature and in the industry-oriented research [1], [2]. In particular, for applications such as uninterruptible power supplies (UPSs), energy-storage systems, variable frequency drives, and distributed generation, the inverters are commonly used with an output *LC* filter to provide a high-quality sinusoidal output voltage with low total harmonic distortion (THD) for various types of loads, especially for unbalanced or nonlinear loads [3]–[6].

The associate editor coordinating the review of this article and approving it for publication was Fan Zhang.

However, the performance of the inverter is mainly dependent on the applied control technique. These controllers must cope with the load variations, the non-linearity of the system, and ensuring stability under any operating condition with a fast transient response [7].

In the literature, various types of classical and modern control schemes have been studied and proposed in order to improve the performance of the converters, such as non-linear methods (e.g., hysteresis voltage control (HVC)) [8], linear methods (e.g., proportional-integral (PI) controller with pulse-width modulation (PWM) and space vector modulation (SVM)) [9]–[12], multi-loop feedback control [13], [14], deadbeat control [15]–[17], repetitive-based controllers [18], [19], linear quadratic controller (LQR) [20], and sliding-mode control [21], [22].

Most of these control schemes, in a way or another, are characterized by a number of limitations. For instance, the major drawback of non-linear methods (e.g., HVC), which require high switching frequency for effective operation, is having a variable switching frequency. This creates resonance problems which reduce the converter's efficiency [23], [24]. On the other hand, although the linear methods, which require carrier-based modulators, have the advantage of constant switching frequency, their dynamic response is weak comparing with HVC, because of the slow response of the modulator. However, both linear and nonlinear methods are extensively used for generating the switching signals of the inverter because of the simplicity of the controller implementation. Another example is deadbeat control which provides fast transient response, but is highly sensitive to model uncertainties, measurement noise, and parameter perturbations, in particular for high sampling rates. Other modern control approaches based on H_∞ control theory [25] and μ synthesis [26] have been proposed, to handle the possible uncertainties in the system.

Model predictive control (MPC) has become one of the well-established modern control methods in power electronics, particularly for three-phase inverters with LC filter according to [1], [23], [27]–[29]. The key characteristic of MPC is to explicitly use the model of the system to predict the future behavior of the variables to be controlled, considering a certain time horizon. Afterwards, MPC selects the optimal control action (i.e., optimal switching signals) based on the minimization of a pre-defined cost function, which represents the desired behavior of the system [30]–[32]. With the aim of getting lower THD and improving steady and dynamic performance, many methods have been proposed in the literature [29], [33]. For instance, the deployment of longer prediction horizons is presented in [34]. However, this results in a significant increase in computational cost. To mitigate and tackle this problem, an improvement of the finite-set FS-MPC strategy, using only a single step prediction horizon, is introduced in [35]. This improvement is mainly based on defining a new cost function, which not only tracks the voltage reference but it also simultaneously tracks its derivative. While, in [36], a current-sensorless FS-MPC scheme for LC-filtered voltage source inverters is proposed, in order to reduce the number of sensors in typical FS-MPC, offering a comparable performance with the typical FS-MPC scheme.

The main features of MPC can be summarized as: (i) an intuitive controller easy to understand and implement, with a fast dynamic response; (ii) no need either for PWM blocks or modulation stage; (iii) the simple inclusion of system constraints and nonlinearities, and multivariable cases; (iv) the flexibility to include other system requirements. On the other hand, a major drawback of MPC is that it requires the optimization problem to be solved online, which involves a huge amount of real-time calculations. However, different solutions have been introduced in order to address this problem, as proposed in [27], [37], [38].

On the other hand, the application of data-driven methodologies (or model-free approaches, particularly artificial neural networks ANNs-based approaches) is currently growing rapidly in the area of power electronics and drives [39]. Broadly speaking, the use of neural networks for the control of dynamical systems was proposed in the early nineties [40]–[42]. Multi-layer perceptrons were employed in various roles, including system identification and implementation of the control law. In particular, ANN-based controllers and estimators have been widely used in identification and control of power converters and motor drives [43]. As an example, they can be used to estimate the rotor speed, rotor-flux, and torque of induction motors [44]–[46], in addition to the identification and estimation of the stator current of induction motor drives [47]. Several ANN-based methods have also been used in the control of power converters, as presented in [48]–[51]. Indeed, the ANN-based controllers have some advantages compared to other control methods such as: (i) their design does not require the mathematical model of the system to be controlled, considering the whole system as a black-box; (ii) they can generally improve the performance of the system when they are properly tuned; (iii) they are usually easier to be tuned as compared to conventional controllers; (iv) they can be designed based on the data acquired from a real system or a plant in the absence of necessary expert knowledge. But, they require a large amount of training data. However, as the present work suggests, this is not a major drawback because data can be obtained using reliable simulation tools.

By taking advantage of the flexibility of MPC at training time, this paper proposes a feed-forward ANN-based controller for a three-phase inverter with output LC filter for UPS applications. The goal is getting lower THD and good performance for different types of loads. The proposed controller undergoes two main steps: (i) we use MPC as an expert or a teacher for generating the data required for training off-line the proposed neural network using standard supervised learning, under full-state observation of the system; (ii) once the off-line training is performed, the trained ANN can successfully control the output voltage of the inverter, without the need of using MPC at test time, as illustrated in Fig. 1. We study a performance comparison between the proposed ANN-based approach and the conventional MPC, under various operating conditions. The main contributions of the work described in this paper can be summarized as follows:

1) To the best of our knowledge, this is the first attempt to directly control a three-phase inverter with an output LC filter using a feed-forward ANN based on MPC, instead of the more common model-based approaches as well as ANN classical control-based (such as Fuzzy Logic Controller FLC-, PID-, or PWM-based) approaches, or a combination of both [49], [52]–[56].

2) The proposed ANN-based approach generates directly the switching signals of the inverter, without the need for the mathematical model of the inverter and without
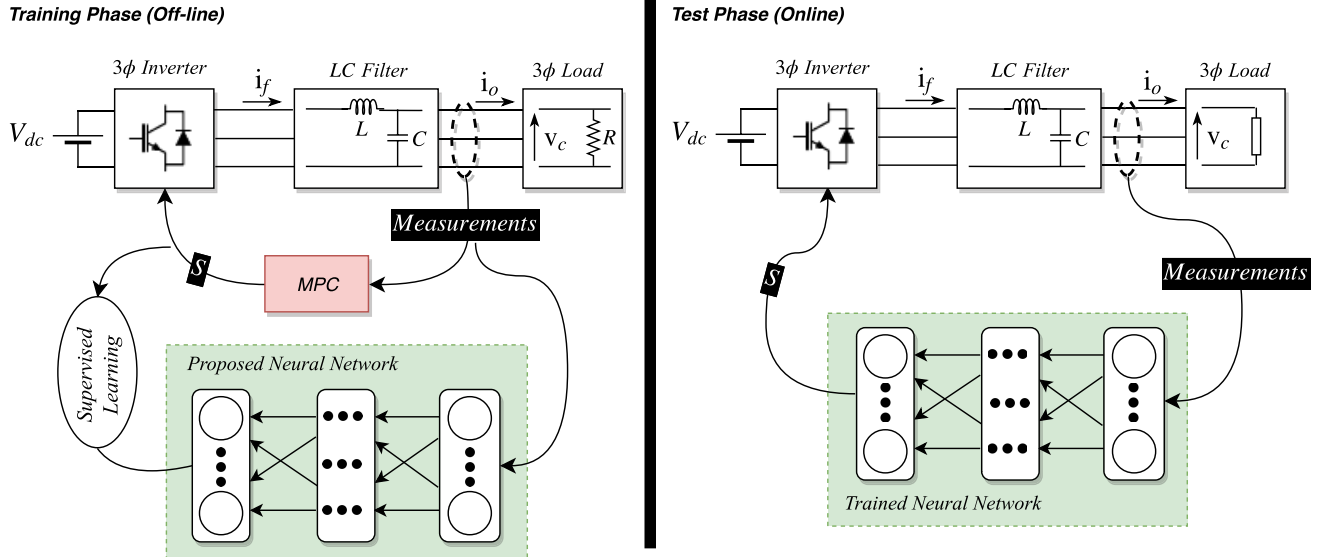
FIGURE 1. An overview of the proposed control strategy: the training phase combines between using MPC for predicting the output voltage of the inverter and collecting data, under full-state observation, for training the neural network. In the test phase, the trained neural network is employed online to control the output voltage of the inverter instead of MPC, considering linear and non-linear loads.

a pre-defined cost function to be minimized at each sampling time T_s. This kind of approach is known as an end-to-end approach.

3) The proposed strategy exhibits very low computational cost compared to [34], [35], with much faster dynamic performance and significantly improved steady-state performance compared to conventional methods.

4) An open repository of the dataset and codes is provided to the community for further research activities.[1]

The rest of the paper is organized as follows. Section II deals with the mathematical model of the three-phase voltage-source inverter with *LC* filter, whereas in Section III the proposed predictive controller strategy is explained. The ANN-based control scheme proposed in this paper is described in Section IV. In Section V, simulation implementation and results are discussed for both proposed control schemes, then the conclusion is provided in Section VI.

II. SYSTEM DESCRIPTION AND MODELING

This section presents the mathematical interpretation of the converter system considered in this paper. The model of *LC* filter is also described in details, and is then used by the predictive controller to predict the output voltage for all given input voltage vectors.

A. SYSTEM DESCRIPTION VIA CLARKE TRANSFORMATION

The power circuit of the three-phase voltage-source inverter considered in this paper is depicted in Fig. 2. In the present case, the load is assumed to be unknown, while the models of the converter and filter are given [57]. Moreover, the two switches of each leg of the converter operate in a complementary mode, in order to avoid the occurrence of short-circuit conditions. Thus, the switching states of the converter can be
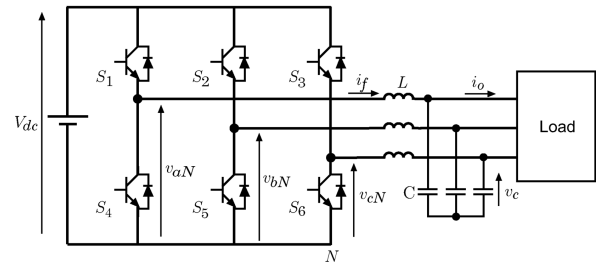
[1] Web: https://github.com/IhabMohamed/ANN-MPC

FIGURE 2. Three-phase voltage-source inverter feeding an output *LC* filter, which is directly connected to either linear or non-linear loads.

represented by the three binary switching signals, S_a, S_b, and S_c, as follows:

$$S_a = \begin{cases} 1, & \text{if } S_1 \text{ ON and } S_4 \text{ OFF} \\ 0, & \text{if } S_1 \text{ OFF and } S_4 \text{ ON} \end{cases}$$

$$S_b = \begin{cases} 1, & \text{if } S_2 \text{ ON and } S_5 \text{ OFF} \\ 0, & \text{if } S_2 \text{ OFF and } S_5 \text{ ON} \end{cases}$$

$$S_c = \begin{cases} 1, & \text{if } S_3 \text{ ON and } S_6 \text{ OFF} \\ 0, & \text{if } S_3 \text{ OFF and } S_6 \text{ ON} \end{cases}$$

These switching states can be expressed in vectorial form (i.e., in $\alpha\beta$ reference frame) by following transformation:

$$\mathsf{S} = \frac{2}{3}(S_a + \mathsf{a}S_b + \mathsf{a}^2 S_c) \equiv \mathsf{S}_\alpha + j\mathsf{S}_\beta,$$

$$\underbrace{\begin{bmatrix} \mathsf{S}_\alpha \\ \mathsf{S}_\beta \end{bmatrix}}_{\mathsf{S}} = \underbrace{\frac{2}{3}\begin{bmatrix} 1 & -1/2 & -1/2 \\ 0 & \sqrt{3}/2 & -\sqrt{3}/2 \end{bmatrix}}_{=:T_c \text{ (Clarke transformation)}} \underbrace{\begin{bmatrix} S_a \\ S_b \\ S_c \end{bmatrix}}_{S_{abc}}, \quad (1)$$

where $\mathsf{a} = e^{j(2\pi/3)}$. The switching devices are assumed to be ideal switches, therefore the process of switching-ON/-OFF is not taken into consideration [28].
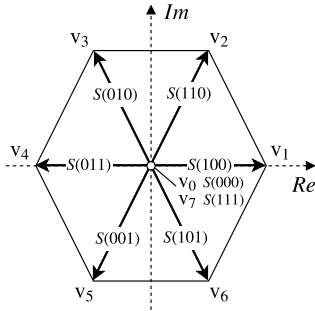
FIGURE 3. Eight possible combinations of the switching signals, and their corresponding voltage vectors generated by the inverter in the complex $\alpha\beta$ frame.

The possible output-voltage space vectors generated by the inverter can be obtained by

$$v_i = \frac{2}{3}(v_{aN} + a v_{bN} + a^2 v_{cN}) \qquad (2)$$

where v_{aN}, v_{bN}, and v_{cN} represent the phase-to-neutral, N, voltages of the inverter. On the other hand, we can define the voltage vector v_i in terms of the switching state vector S and the dc-link voltage V_{dc} by

$$v_i = V_{dc} S. \qquad (3)$$

Fig. 3 illustrates the eight switching states and, consequently, the eight voltage vectors generated by the inverter using (1) and (3), considering all the possible combinations of the switching signals S_a, S_b, and S_c. It is noteworthy that only seven different voltage vectors are considered as possible outputs, since $v_0 = v_7$.

Similarly, as in (1), the filter current i_f, the output voltage v_c, and the output current i_o can be expressed in vectorial form as

$$i_f = \frac{2}{3}(i_{fa} + a i_{fb} + a^2 i_{fc}) \equiv i_{f\alpha} + j\,i_{f\beta}, \qquad (4)$$

$$v_c = \frac{2}{3}(v_{ca} + a v_{cb} + a^2 v_{cc}) \equiv v_{c\alpha} + j\,v_{c\beta}, \qquad (5)$$

$$i_o = \frac{2}{3}(i_{oa} + a i_{ob} + a^2 i_{oc}) \equiv i_{o\alpha} + j\,i_{o\beta}. \qquad (6)$$

B. LC FILTER MODELING

The model of *LC* filter can be described by two equations: the former describes the inductance dynamics, whereas the latter describes the capacitor dynamics [1]. These two equations can be written as a continuous-time state-space system as

$$\frac{dx}{dt} = Ax + Bv_i + B_q i_o,$$

$$\frac{d}{dt}\underbrace{\begin{bmatrix} i_f \\ v_c \end{bmatrix}}_{x} = \underbrace{\begin{bmatrix} 0 & -\dfrac{1}{L} \\ \dfrac{1}{C} & 0 \end{bmatrix}}_{A} \underbrace{\begin{bmatrix} i_f \\ v_c \end{bmatrix}}_{x} + \underbrace{\begin{bmatrix} \dfrac{1}{L} \\ 0 \end{bmatrix}}_{B} v_i + \underbrace{\begin{bmatrix} 0 \\ -\dfrac{1}{C} \end{bmatrix}}_{B_q} i_o,$$

$$\qquad (7)$$

where L and C are the filter inductance and the filter capacitance, respectively. The output voltage v_c and the filter current i_f can be measured, whilst the voltage vector v_i can be calculated using (3). The output current i_o is considered as a disturbance due to its dependence on an unknown load, whereas the value of V_{dc} is assumed to be fixed and known. The output voltage v_c is considered as the output of the system, which can be written as a state equation as $v_c = \begin{bmatrix} 0 & 1 \end{bmatrix} x$.

Then, using (7), the discrete-time state-space model of the filter can be obtained for a sampling time T_s as

$$x(k+1) = A_q x(k) + B_q v_i(k) + B_{dq} i_o(k),$$

$$\underbrace{\begin{bmatrix} i_f(k+1) \\ v_c(k+1) \end{bmatrix}}_{x(k+1)} = \underbrace{e^{AT_s}}_{A_q} \underbrace{\begin{bmatrix} i_f(k) \\ v_c(k) \end{bmatrix}}_{x(k)} + \underbrace{\int_0^{T_s} e^{A\tau} B\, d\tau}_{B_q}\, v_i(k)$$

$$+ \underbrace{\int_0^{T_s} e^{A\tau} B_d\, d\tau}_{B_{dq}}\, i_o(k). \qquad (8)$$

This model is used by the predictive controller (i.e., MPC) to predict the output voltage v_c for all given input voltage vectors v_i. Then, for predicting the output voltage v_c using (8), we need the output current i_o which can be estimated using (9), assuming that $i_o(k-1) = i_o(k)$ for sufficiently small sampling times T_s as proposed in [1], [34].

$$i_o(k-1) \cong i_o(k) = i_f(k-1) - \frac{C}{T_s}\Big(v_c(k) - v_c(k-1)\Big) \qquad (9)$$

III. MODEL PREDICTIVE CONTROL FOR NEURAL NETWORK

In this section we employ the model predictive control (MPC) proposed in [31], [57], which provides the state-of-art of output-voltage control of three-phase inverter for UPS applications, for two purposes: (i) to generate the data required for the off-line training of the proposed neural network, and (ii) to compare its performance with the proposed ANN-based controller under linear and non-linear load conditions.

A. PROPOSED PREDICTIVE CONTROLLER STRATEGY

In the proposed control strategy, we assume that the inverter generates only a finite number of possible switching states and their corresponding output-voltage vectors, making it possible to solve the optimization problem of the predictive controller online [1]. MPC exploits the discrete-time model of the inverter to predict the future behavior of the variables to be controlled, for each switching state. Thereafter, the optimum switching state is selected, based on the minimization of a pre-defined cost function, and directly fed to the power switches of the converter in each sampling interval T_s, without the need for a modulation stage. We choose the cost function to be minimize so as to achieve the lowest error between the predicted output voltage and
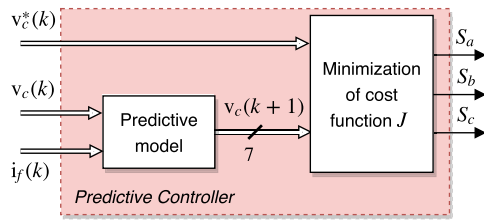
FIGURE 4. Schematic diagram of the MPC scheme for a three-phase inverter with an output *LC* filter. The controller takes the measured variables i_f, v_c, and v_c^* as inputs, while the switching signals S_a, S_b, and S_c constitute the outputs.

the reference voltage. We express the cost function J, which defines the desired behavior of the system, in orthogonal coordinates by

$$J = \left(v_{c\alpha}^* - v_{c\alpha}(k+1) \right)^2 + \left(v_{c\beta}^* - v_{c\beta}(k+1) \right)^2 \quad (10)$$

where $v_{c\alpha}^*$ and $v_{c\beta}^*$ are the real and imaginary parts of the output-voltage reference vector v_c^*, while $v_{c\alpha}$ and $v_{c\beta}$ are the real and imaginary parts of the predicted output-voltage vector $v_c(k+1)$.

The block diagram of MPC, considering only one-step prediction horizon, for a three-phase inverter with output *LC* filter is shown in Fig. 4. The control cycle of the predictive controller at sampling instant k is described as a pseudo code in Algorithm 1 with more detail. Line 1 of the code declares the control function, where the switching signals S_a, S_b, and S_c are the outputs, while the inputs are the measured variables of the filter current $i_f(k)$, the output voltage $v_c(k)$, and the reference voltage $v_c^*(k)$ at sampling time k, all expressed in $\alpha\beta$ coordinates. The two variables, $i_f(k-1)$ and $v_c(k-1)$, are recalled from the previous sampling instant (lines 7 to 9), which are firstly initialized for $k = 1$ (lines 3 to 6). These two variables are used to estimate the output current $i_o(k)$ given by (9) (line 10), in order to obtain the possible predictions of $v_c(k+1)$ using (8).

The optimization is performed between lines 12 and 20. The code sequentially selects one of the seven possible voltage vectors v_i generated by the inverter based on (3) (line 13) and applies it, in order to obtain the output voltage prediction $v_c(k+1)$ at instant $k+1$, as in line 14. The cost function given by (10) is used to evaluate the error between the reference and the predicted output voltage at instant $k+1$ for each voltage vector (line 15). The code selects the *optimal* value of the cost function J_{opt}, and the *optimum* voltage vector x_{opt} is then chosen (lines 16 to 19). Note that J_{opt} is initialized with a very high value (line 11). Finally, the switching states, S_a, S_b, and S_c, corresponding to the *optimum* voltage vector are generated and applied at the next sampling instant (line 22), as illustrated in Fig. 3.

B. DISCUSSION
We can observe that all the control approaches proposed in the literature, in a way or another, are model-based approaches, which require in general either diverse computational or approximative procedures for applying their solution. In this context, MPC, the widely used approach

---

Algorithm 1 Pseudo Code of the MPC Scheme [31]

1: **function** $[S_a, S_b, S_c] = MPC(i_f(k), \mathbf{v}_c(k), \mathbf{v}_c^*(k))$
2:     Measure the first sampled values as $i_f(1), v_c(1), v_c^*(1)$;
3:     **if** $k = 1$ **then**
4:         Set $i_f(k-1) = i_f(0) = 0 + j0$;
5:         Set $v_c(k-1) = v_c(0) = 0 + j0$;
6:     **end if**
7:     **if** $k > 1$ **then**
8:         Recall measured variables $i_f(k-1), v_c(k-1)$;
9:     **end if**
10:    Estimate $i_o(k) = i_f(k-1) - \frac{C}{T_s}\left(v_c(k) - v_c(k-1) \right)$;
11:    Set $J_{opt} = \infty$;
12:    **for** $l = 1$ to 7 **do**
13:       Compute $v_i(l) = S(l)V_{dc}$;
14:       Predict $v_c(k+1)$ at instant $k+1$ using (8);
15:       Evaluate $J = \left(v_c^*(k) - v_c(k+1) \right)^2$;
16:       **if** $J(l) < J_{opt}$ **then**
17:          Set $J_{opt} = J(l)$;
18:          Set $x_{opt} = l$;
19:       **end if**
20:    **end for**
21:    Set $S_{opt} = S(x_{opt})$;
22:    **return** $[S_a, S_b, S_c] = [S_{opt}(1), S_{opt}(2), S_{opt}(3)]$;
23: **end function**

---

for three-phase inverters, relies on solving an optimization problem online, leading to a large number of online computations. In other words, the control signal of MPC is determined by minimizing a cost function online at each time instant. Recently artificial neural networks have been used in conjunction with MPC, in order to provide a powerful and fast optimization as proposed in [58]–[61].

The alternative approach considered in the present work is to apply neural network-based function approximators, which can be trained off-line to represent the optimal control law. Such an approach is expected to avoid the drawbacks associated with MPC-based control approaches, does not require the mathematical model of the system to be controlled, does not evaluate a cost function online at each sampling time, and, therefore, does not rely on an optimization problem to be solved online. For this reason, this paper focuses on the control of a three-phase inverter with output *LC* filter using a feed-forward ANN-based MPC, which has not been reported in the literature, where MPC is only used as a teacher for training the neural network.

IV. IMPLEMENTATION OF ANN-BASED CONTROLLER
In this section, some important concepts related to ANN including the structure of the proposed ANN-based controller as well as details on the training data will be covered.

A. PROPOSED NEURAL NETWORK ARCHITECTURE

Machine learning, and in particular artificial neural networks, is one key technology in modern control systems. An artificial neural network (ANN) is an extremely flexible computational model that can be optimized to learn input-to-output mappings based on historical data. An ANN is composed of a number of simple computing elements linked by weighted connections. Feed-forward networks do not contain loops, so they are organized in layers and can be used to implement input-to-output mappings that are memoryless, i.e., without dynamics. In its basic form, this model can be expressed as an iterative composition of input-output functions of the form

$$f(\vec{x}) = h\left(w_0 + \sum_{i=1}^{M} w_i x_i\right), \qquad (11)$$

where $h(x)$ is an activation function (usually it is a non-linear function such as *logistic sigmoid* or *hyperbolic tangent*, to ensure the universal approximation property [62]), $\vec{x} = \{x_1, x_2, \cdots, x_M\}$ is the input vector of the ANN with M elements, w_i are the weights for each input x_i, and w_0 is a bias or correction factor. In a feed-forward network, it is possible to distinguish one input layer, one output layer, and hidden layers that connect the input to the output. The objective of the ANN training phase is to optimize some cost function by finding optimal values for the w_i and w_0.

Although recent developments have focused on larger and larger scale problems (deep learning), improved techniques have also been proposed to improve the reliability of networks of smaller size. Toward the same goal, hardware suppliers have started to support reduced-precision floating-point [63] and integer [64] arithmetics, and offer small-scale, dedicated architectures [65]. The result is a sound and scalable technology.

In this work, a feed-forward neural network (fully connected multi-layer perceptron) of the "shallow" type, i.e., one hidden layer, was used to implement the control model. A grid search tuning procedure allowed the selection of a configuration with 15 units in the hidden layer, while the number of input and output units is constrained by the number of input and output variables, respectively. Training was done via the Scaled Conjugate Gradient (SCG) method [66], which exploits the good convergence properties of conjugate gradient optimization [67] and has the computational advantage of not requiring a line search, nor any user-selected parameters.

B. ANN TRAINING PROCEDURE

The ANN takes as inputs the measured variables of the filter current i_f, the output voltage v_c, the output current i_o, and the reference voltage v_c^* all expressed in $\alpha\beta$ coordinates. The real and imaginary parts of these variables are separately fed to the neural network, bringing the total number of input features to eight, i.e., $M = 8$. The output of the ANN is the *optimum* voltage vector x_{opt} to be applied at each sampling instant. The size of the output layer is an array with a length of 7, which represents the indexes of the seven possible voltage

TABLE 1. Training results of the proposed ANN based on 60 and 70 training cases, which have been collected by MPC.

Tr. Cases	No. of Instances	Accuracy	Validation Error (epoch)
60	217, 510	69.1%	0.11108 (747)
70	247, 820	69.3%	0.11213 (526)

vectors v_i that inverter generates. The output is one-hot encoded, meaning that at each sampling instant only the index of the *optimum* voltage vector will be active (i.e., having a value of one), while others will be equal to zero.

The training data, which have been collected by MPC, comprises 70 experimental conditions, which are divided into 60 cases for specific resistive loads (i.e., for only $R = 1, 3, 5, 7, 10, 15, 20, 25, 30,$ and $35 \ \Omega$), whereas only 10 experiments represent the case where the inverter directly feeds a non-linear load (i.e., diode-bridge rectifier) with different values of R_{NL} and C_{NL}. For each experimental condition, the simulation is run using MPC,[2] under various operating conditions such as simulation time (i.e, number of output voltage cycles), sampling time T_s, filter capacitor C, filter inductance L, DC-link voltage V_{dc}, and reference voltage v_c^*. Then, the input features of the neural network and their targets are stored for training.

As a consequence, the total dataset consists of 217, 510 and 247, 820 instances for the cases where 60 and 70 experimental conditions are used, respectively. These dataset has been divided into two parts: 70% randomly selected for training purposes, and 30% for testing and validation. The overall accuracy of ANN for the 60 training cases is 69.1%, while it has a 0.2% increase for the 70 training cases, considering 15 hidden layers and the training function "*transcg*". We observe that the validation and training error, as well as the error on the test set, are very similar when training stops, according to the "*early stopping*" criterion used. This is an indication that the neural network may attain a good degree of generalization. For instance, for the 60 training cases, the best validation performance is taken from epoch 747 with the lowest validation error of 0.11108. The training results are summarized in Table 1. Training was also attempted using the Bayesian regularization back-propagation method, achieving an accuracy of 93%. However, its performance at the test phase (on-line) was not satisfactory.

For further detailed information about the training cases used for training the ANN-based controller, please refer to: https://github.com/IhabMohamed/ANN-MPC.

C. ANN-BASED CONTROLLER

As previously mentioned, the ANN-based controller is trained off-line from samples collected via MPC, as shown in Fig. 1. After fine-tuning the ANN, the trained ANN can be used instead of MPC to control the system presented in Fig. 2.

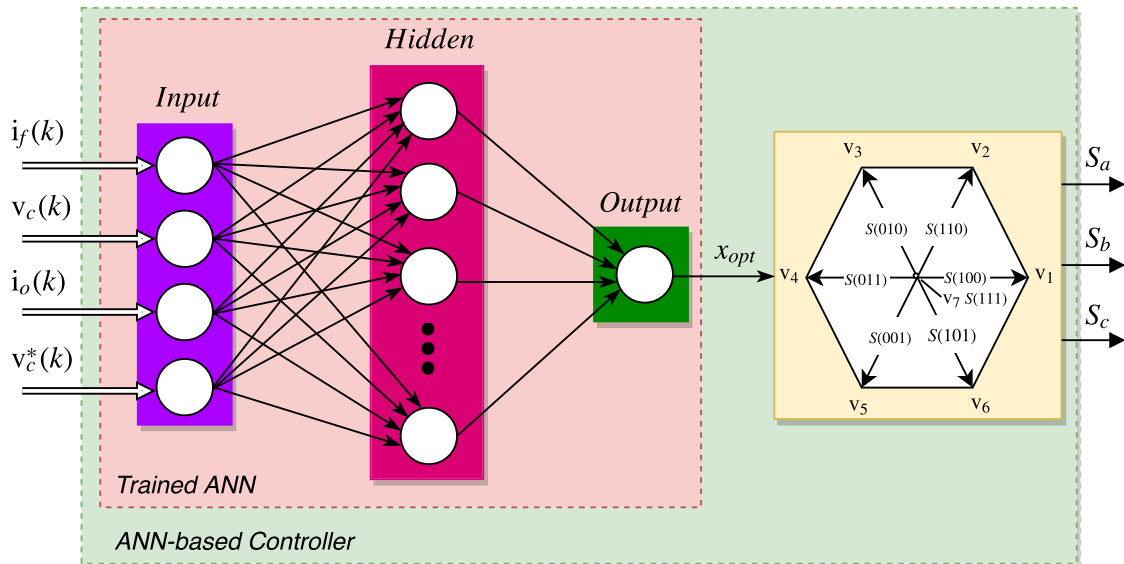Fig. 5 depicts the proposed block diagram of the ANN-based controller for a three-phase inverter with output

---

[2]Web: https://github.com/IhabMohamed/MPC-3-Phase-Inverters

FIGURE 5. Block diagram of the proposed ANN-based controller for a three-phase inverter with an output *LC* filter. Each sampling instant, the trained ANN takes, as input, the measured variables i_f, v_c, i_o, and v_c^*, whereas it explicitly generates the *optimum* voltage vector x_{opt}. Afterwards, the corresponding switching states S_a, S_b, and S_c are directly given to the power switches of the converter.

LC filter, in order to generate a high-quality sinusoidal output voltage with low THD, considering different types of loads.

The control strategy of the proposed ANN-based controller at sampling time k can be described as follows:

1) measure the value of the filter current $i_f(k)$, the output voltage $v_c(k)$, and the output current $i_o(k)$ at sampling time k. Note that, the output current $i_o(k)$ is considered to be a measurable value, without estimation based on (9) or using the observer as in [1];

2) then, these measured values in addition to the reference voltage $v_c^*(k)$ are used by the trained ANN in order to explicitly generate the *optimum* voltage vector x_{opt} to be applied at instant $k + 1$;

3) finally, the switching states, S_a, S_b, and S_c, corresponding to the optimum voltage vector x_{opt} are applied and directly given to the power switches of the converter each sampling interval T_s.

V. SIMULATION IMPLEMENTATION AND RESULTS

This section provides a comprehensive study and evaluation of the two proposed control strategies, taking into account different loads under various operating conditions.

A. SIMULATION SETUP

To verify the proposed ANN-based control strategy and compare its performance with the conventional MPC, we used MATLAB (R2018a)/Simulink software components to implement the Simulink model and the simulations of the system shown in Fig. 2. We acquired the training samples, off-line training, and online voltage tracking purpose using the proposed ANN approach via a PC equipped with an Intel® Core i5-4210U 1.70 *GHz* CPU, 6 GB of RAM, and an Nvidia Geforce® GPU, and running Ubuntu 16.04 64 bit.

TABLE 2. Parameters of the converter system.

Parameter	Value
DC-link voltage V_{dc}	500 [V]
Filter capacitor C	40 [μF]
Filter inductance L	2 [mH]
Sampling time T_s	30 [μs]

B. SIMULATION RESULTS

The simulation of the three-phase inverter system shown in Fig. 2 was carried out, considering linear (i.e., resistive) and non-linear loads, in order to evaluate the behavior of the proposed ANN-based control strategy and compare its performance with that of MPC proposed in Section III. In particular, we studied and evaluated the steady and dynamic performance of both control strategies, taking into account different loads conditions. The parameters of the system are listed in Table 2.

The behavior of the ANN-based controller in steady-state operation for a resistive load of 5 kΩ shown in Fig. 6, while the behavior of the predictive controller for the same resistive load is shown in Fig. 7. The amplitude and the fundamental frequency of reference voltage v_c^* are set to 200 V and 50 Hz, respectively. It can be seen in the figures that the output voltages v_c for the proposed control strategies are sinusoidal with low distortion, particularly for the ANN-based approach which has a THD of only 1.6% compared to 3.95% for MPC. Moreover, we observe that, due to the resistive load, the output current i_o is proportional to the output voltage, whilst the filter current i_o measured at the output of the converter shows high-frequency harmonics, especially in the case of MPC, which are attenuated by the *LC* filter.

The transient response of both control strategies for no-load (i.e., open-circuit) is shown in Fig. 8 and Fig. 9. Here, the filter capacitor C and filter inductance L are set to 50 μF
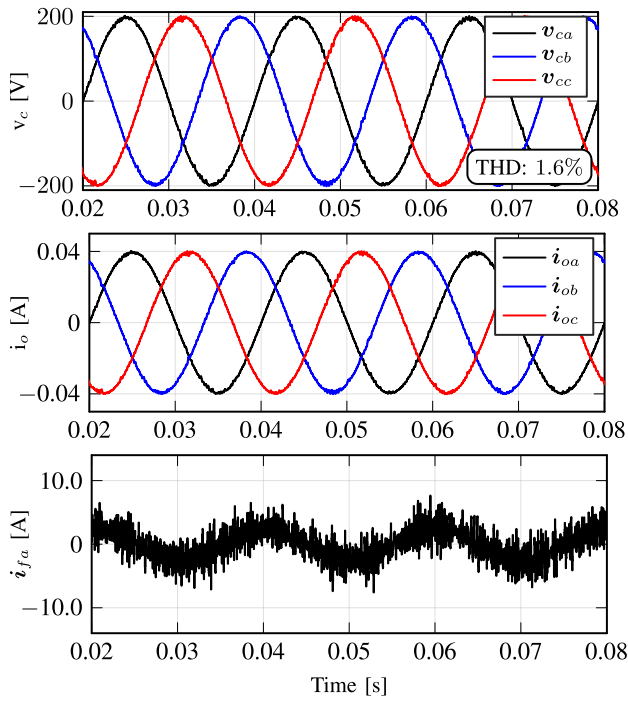
FIGURE 6. Simulation results of ANN-based controller: output voltages, output currents, and filter current in steady-state for a resistive load of $5\,\text{k}\Omega$.
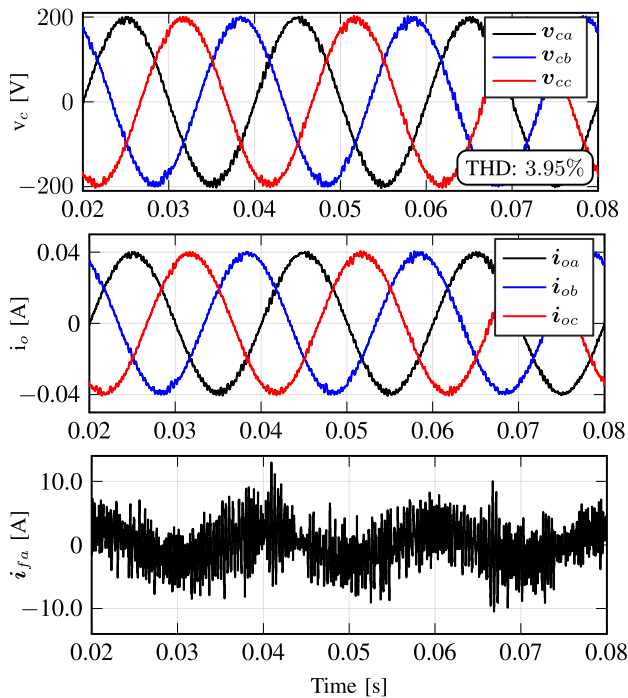

FIGURE 7. Simulation results of MPC: output voltages, output currents, and filter current in steady-state for a resistive load of $5\,\text{k}\Omega$.

and $3.5\,\text{mH}$, respectively, whilst the sampling time T_s is kept constant at a value of $30\,\mu\text{s}$. It can be seen that the ANN-based controller permits a fast and safe transient response, demonstrating the excellent dynamic performance of the
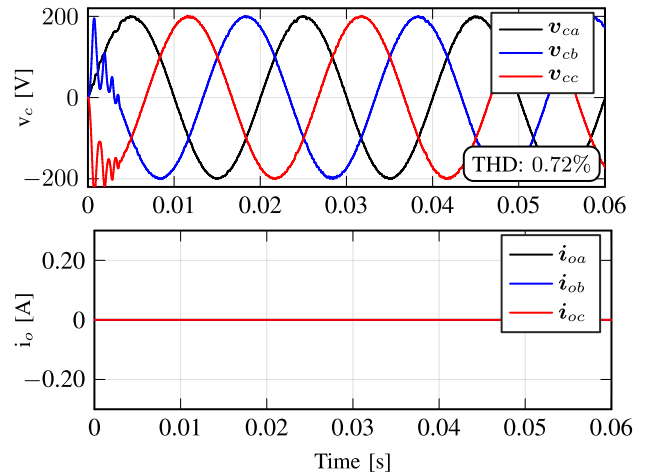

FIGURE 8. Simulation results: the dynamic response of the ANN-based controller for a no-load, where the filter capacitor $C = 50\,\mu\text{F}$, the filter inductance $L = 3.5\,\text{mH}$, and $T_s = 30\,\mu\text{s}$.
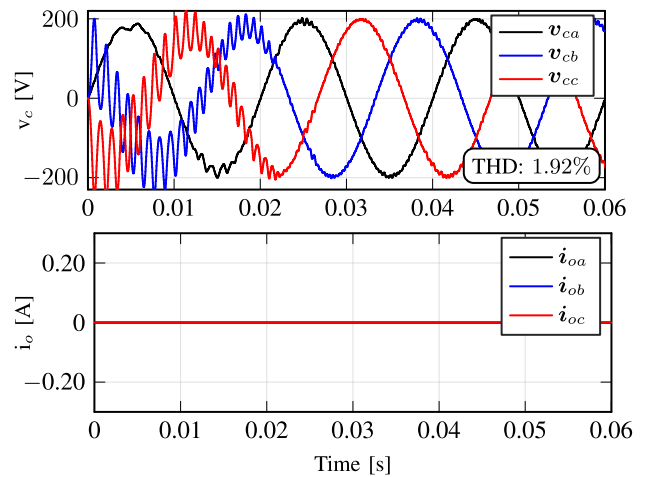
FIGURE 9. Simulation results: the dynamic response of MPC for a no-load, where the filter capacitor $C = 50\,\mu\text{F}$, the filter inductance $L = 3.5\,\text{mH}$, and $T_s = 30\,\mu\text{s}$.

proposed ANN-based control strategy. For MPC, the time elapsed in order to reach steady-state operation and to faithfully track its reference waveform is about $20\,\text{ms}$ (1 *cycle*), which is affected by the change in the load, as illustrated in Table 3. On the other side, for the ANN-based controller, it is observed that it takes less than $5\,\text{ms}$ for any load, in order to reach steady-state. Furthermore, the output voltage quality of ANN-based approach is improved significantly, with a THD of 0.72% compared to 1.92% for MPC.

As previously mentioned, the proposed ANN is trained off-line using a dataset which represents only different values of resistive load under different operating conditions. However, to verify the feasibility and effectiveness of the proposed ANN-based controller under realistic conditions, the behavior of the system is tested online considering non-linear loads, such as a diode-bridge rectifier as shown in Fig. 10 and an inductive load. Fig. 11 and Fig. 12 show

TABLE 3. A comparison between the two proposed control strategies for linear and non-linear loads under different operating conditions such as sampling time *Ts*, filter capacitor *C*, filter inductance *L*, DC-link voltage *Vdc*, and reference voltage *vc***.

Case # 1: Resistive Load as Linear Load with R							Results		
							$(\text{THD})_{\text{ANN}}$ [%]		$(\text{THD})_{\text{MPC}}$ [%] (t_{ss})
Sample No.	R [Ω]	T_s [μs]	L [mH]	C [μF]	V_{dc} [V]	v_c^* [V]	$(\text{THD})_{S_1-S_{60}}$	$(\text{THD})_{S_1-S_{70}}$	
S_1	10	25	2.5	50	550	250	**0.49**	0.52	1.16 (2 ms)
S_2	30	25	2.5	50	520	200	**0.55**	0.57	1.46 (5 ms)
S_3	50	25	2.5	50	500	250	**0.65**	0.68	1.59 (5 ms)
S_4	80	25	2.5	50	500	150	**0.66**	0.70	1.58 (10 ms)
S_5	300	25	2.0	50	450	200	**0.63**	0.65	2.32 (20 ms)
S_6	500	25	2.0	40	550	250	**0.95**	1.06	2.84 (35 ms)
S_7	1 kΩ	25	3.5	40	520	200	0.72	**0.70**	1.51 (35 ms)
S_8	2 MΩ	25	4.0	40	500	150	**0.76**	0.84	1.31 (30 ms)
S_9	10 MΩ	25	2.0	40	500	200	0.99	**0.98**	2.61 (10 ms)
S_{10}	Open Circuit	25	3.5	40	450	150	**0.79**	0.83	1.15 (30 ms)
S_{11}	15	30	2.5	50	550	250	**0.72**	0.74	1.75
S_{12}	40	30	2.5	50	520	200	0.86	**0.83**	2.04
S_{13}	100	30	2.5	50	500	250	**0.88**	1.12	2.36
S_{14}	200	30	2.5	50	500	150	0.98	**0.95**	2.40
S_{15}	300	30	2.0	50	450	200	**0.96**	0.99	3.33
S_{16}	500	30	2.0	40	500	200	**1.58**	1.82	3.49
S_{17}	2 kΩ	30	3.5	40	520	200	1.15	**1.09**	2.36
S_{18}	1 MΩ	30	4.0	40	500	150	**1.20**	1.27	1.88
S_{19}	5 MΩ	30	2	40	500	200	**1.61**	1.62	3.91
S_{20}	Open Circuit	30	2.0	40	450	250	**2.25**	2.25	5.34
S_{21}	20	35	2.5	50	550	250	**1.11**	1.21	2.67
S_{22}	100	35	2.0	50	520	200	**1.66**	1.66	3.85
S_{23}	250	35	3.5	40	500	150	**2.10**	2.33	2.92
S_{24}	400	40	2.5	50	500	200	**2.27**	2.48	4.11
S_{25}	500	40	4.0	45	450	200	**1.50**	1.89	2.91
S_{26}	400	40	2.5	40	500	200	5.40	4.87	**4.42**
S_{27}	3 kΩ	35	2.0	40	550	200	4.23	4.30	**4.19**
S_{28}	3 kΩ	40	2.0	40	500	150	8.44	8.87	**5.63**
S_{29}	1 MΩ	35	3.0	35	500	200	4.66	4.81	**3.61**
S_{30}	Open Circuit	40	3.5	40	450	150	5.39	5.15	**3.70**

Case # 2: Diode-Bridge Rectifier as Non-Linear Load with R_{NL} and C_{NL}								Results		
								$(\text{THD})_{\text{ANN}}$ [%]		$(\text{THD})_{\text{MPC}}$ [%]
Sample No.	R_{NL} [Ω]	C_{NL} [μF]	T_s [μs]	L [mH]	C [μF]	V_{dc} [V]	v_c^* [V]	$(\text{THD})_{S_1-S_{60}}$	$(\text{THD})_{S_1-S_{70}}$	
S_{31}	10	3000	25	2.4	50	520	200	**3.97**	3.97	7.44
S_{32}	30	3000	25	3.5	50	500	200	**1.99**	2.10	3.80
S_{33}	60	3000	25	2.0	50	500	250	**1.97**	1.98	2.76
S_{34}	1 kΩ	3000	25	2.4	40	550	150	0.97	**0.94**	2.11
S_{35}	1 kΩ	200	25	3.5	35	520	200	**0.80**	0.90	1.40
S_{36}	60	100	25	4.0	40	450	150	1.36	**1.30**	1.64
S_{37}	100	1000	25	2.5	30	520	250	**2.22**	2.47	2.98
S_{38}	20	2000	33	3.0	50	520	200	**2.94**	3.10	4.57
S_{39}	30	2000	33	3.5	40	500	200	3.77	**3.32**	3.69
S_{40}	60	2000	33	2.0	50	500	250	**3.15**	3.31	4.08
S_{41}	2 kΩ	3000	33	2.4	40	550	150	2.90	**2.89**	3.65
S_{42}	2 kΩ	200	33	3.5	35	520	200	2.22	**2.19**	2.55
S_{43}	60	100	33	4.0	40	450	150	**1.69**	1.74	1.97
S_{44}	80	1000	33	4.0	35	520	250	**3.47**	3.60	3.66
S_{45}	100	3000	40	3.5	50	500	200	**2.04**	2.22	2.92
S_{46}	900	3000	40	3.0	40	520	250	4.32	**4.30**	4.65
S_{47}	100	1000	40	4.0	50	450	200	2.73	**2.70**	2.84
S_{48}	100	5000	40	4.0	45	520	250	3.71	3.79	**3.63**
S_{49}	1 kΩ	3000	40	2.5	35	500	150	22.23	21.50	**5.78**
S_{50}	1 kΩ	3000	40	2.5	50	500	150	2.41	**2.30**	4.76

the behavior of the proposed control strategies for a diode-bridge rectifier, with values $C = 300\,\mu\text{F}$ and $R = 60\,\Omega$, while the behavior for an inductive load of 0.01 H is shown in Fig. 13 and Fig. 14, considering the same operating conditions presented in Table 2 and different amplitudes of the reference output voltage. As can be seen in the figures, the output voltage generated by the ANN-based controller outperforms that obtained using MPC for non-linear loads, despite the highly distorted output currents due to feeding a non-linear load. For instance, for MPC, the total distortion in
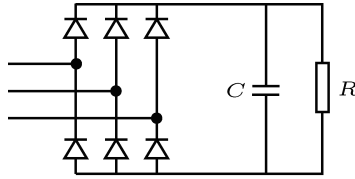
FIGURE 10. Diode-bridge rectifier used as non-linear load, with values $C = 300\,\mu\text{F}$ and $R = 60\,\Omega$.
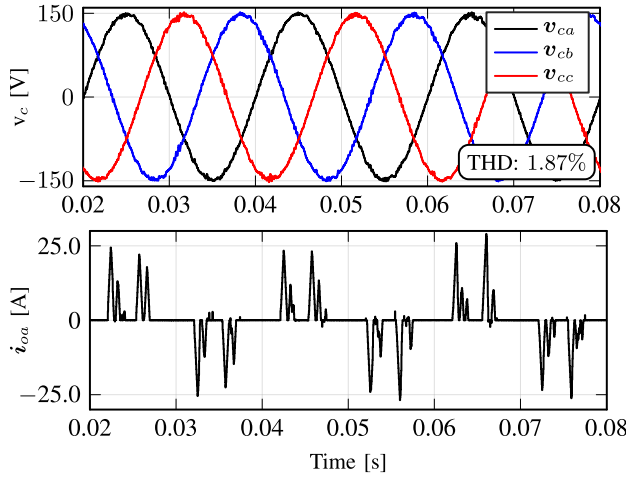

FIGURE 11. Simulation results of ANN-based controller: output voltages and one-phase output current in steady-state for a diode-bridge rectifier and a reference amplitude of $150\,\text{V}$.
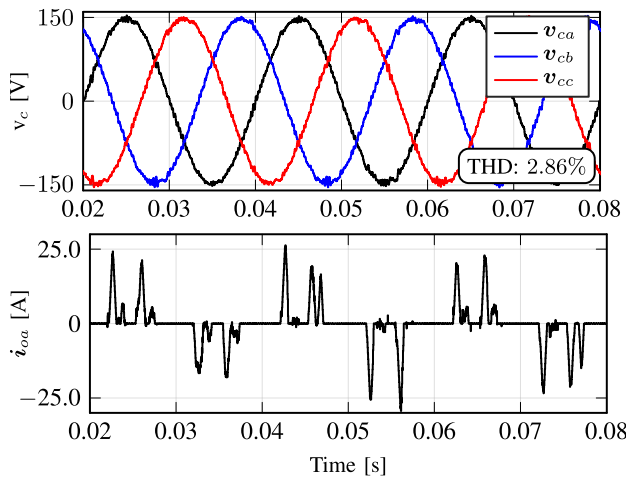

FIGURE 12. Simulation results of MPC: output voltages and one-phase output current in steady-state for a diode-bridge rectifier and a reference amplitude of $150\,\text{V}$.

FIGURE 13. Simulation results of ANN-based controller: output voltages in steady-state for an inductive load of $0.01\,\text{H}$ and a reference amplitude of $200\,\text{V}$.

FIGURE 14. Simulation results of MPC: output voltages in steady-state for an inductive load of $0.01\,\text{H}$ and a reference amplitude of $200\,\text{V}$.

the output voltage for the inductive load was 4.86%, while it was 2.2% for the ANN-based controller. The result of MPC can be improved by using either a smaller sampling time or a higher value of the filter capacitance [28].

In order to achieve a fair comparison and prove the superiority of the proposed ANN-based approach compared to MPC in both transient and steady-state response, Table 3 shows a comprehensive comparison of both the control
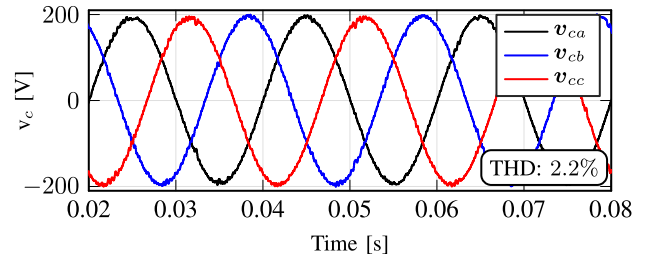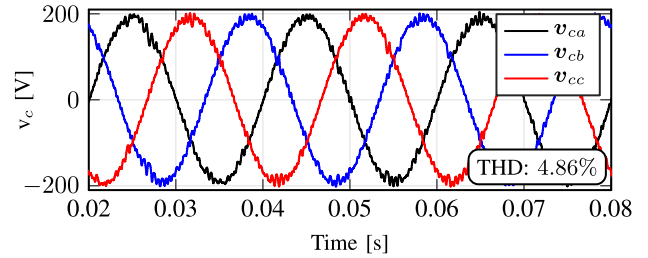
strategies for linear and non-linear loads, under various operating conditions such as sampling time T_s, filter capacitor C, filter inductance L, DC-link voltage V_{dc}, and reference voltage v_c^*. Fifty unseen cases, at training time, have been considered for testing the proposed approaches, including thirty cases for different values of a resistive load, whereas the rest was for a diode-bridge rectifier as a non-linear load. Moreover, the THD of the output voltage obtained by the proposed control strategies, for some cases given in Table 3, is visualized in Fig. 15. As anticipated, the performance of the ANN-based approach, either based on sixty or seventy training cases, outperforms that of MPC, which can be noticed in lower THD and less settling time to reach steady-state (i.e., t_{ss}, as shown in the first ten samples (i.e., $S_1 - S_{10}$)). It can be noticed that the performance of the ANN-based controller using only sixty training cases is similar to that based on seventy cases (see column 8 and 9 in Table 3).

However, for cases $S_{26} - S_{30}$, the output voltages obtained using MPC are better than that obtained using the ANN-based controller. Moreover, it can be seen in sample S_{49} that the ANN-based approach failed to control the output voltage and track its reference waveform. As a consequence, the UPS does not work properly due to a higher distortion in the voltage. These results could be improved using either (i) a higher sampling frequency, or (ii) a higher value of the filter capacitance C, as illustrated in sample S_{50} which represents an improvement of the result of sample S_{49}. An alternative solution to be considered to improve the performance of the controller is to increase the number of training instances, taking into account various values of C and T_s. In addition, it is observed that having a one-delay step in the input features of the neural network improves
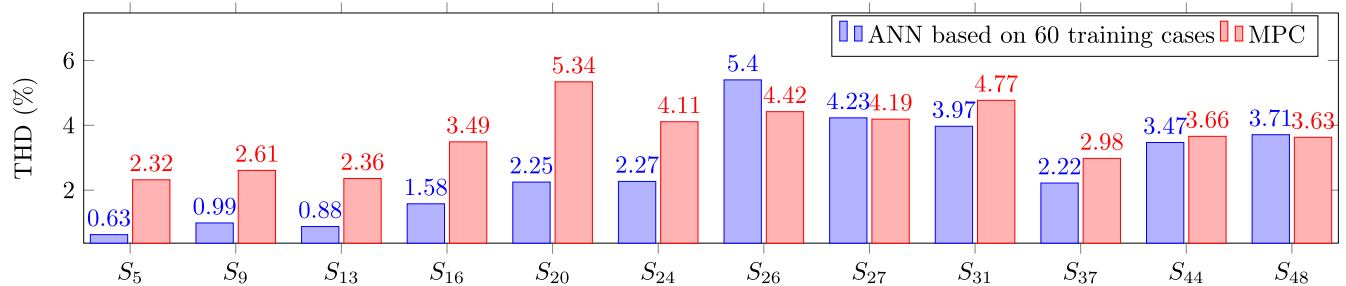
FIGURE 15. Comparison of the THD of the output voltage obtained by the two proposed control strategies, for some cases given in Table 3, under different operating conditions.

its performance to outperform that of MPC. For example, $(THD)_{ANN}$ of cases $S_{26}, S_{27}, S_{28}, S_{29}, S_{49}$ is decreased to be 3.72%, 2.39%, 4.08%, 2.35%, 3.86%, respectively.

In fact, it is not surprising that the performance of the proposed ANN-based controller outperforms that of MPC in both transient and steady-state response, even with unseen experimental conditions (i.e., loads) at training time as tabulated in Table 3. This happened for two reasons. First, the training data are sufficient to learn the mathematical model of the system to be controlled and its dynamics, as well as representing the optimal control law. Second, generating a sinusoidal output voltage can be considered as a repetitive task, where neural network can easily detect and learn repetitive sequences of actions.

At the moment, one can say that the main limitation of the proposed method is that only the simulation results are not sufficient to prove its novelty in practical applications. However, indeed we believe that our proposed approach will also represent a novel contribution to the practical applications for the following reasons: (i) based on the previously proposed literature, both ANN-based and MPC-based approaches have shown good results in both simulated and experimental scenarios; (ii) moreover, the trained network is only required to be fine-tuned, in order to improve its performance in practical applications.

VI. CONCLUSION AND FUTURE WORK

A novel control strategy using a feed-forward ANN to generate a high-quality sinusoidal output voltage of a three-phase inverter with an output *LC* filter has been successfully developed and tested, for different types of loads under various operating conditions. The output voltage of the inverter is directly controlled, without the need for the mathematical model of the inverter, considering the whole system as a black-box. In this work, MPC has been used for two main purposes: (i) generating the data required for the off-line training of the proposed ANN, and (ii) comparing its performance with the proposed ANN-based controller for linear and non-linear load conditions. Simulation results, based on fifty test different than those that were used at training time, show that the proposed ANN-based controller performs better than MPC, in terms of a lower THD and a fast and safe

transient response, demonstrating the excellent steady and dynamic performance of the proposed ANN-based control strategy. As in any model-based control strategy, variations in the system parameters inevitably influence the performance of the ANN-based control scheme proposed in this paper. The possible directions for future work would be (i) the implementation of the ANN-based controller in practical applications; then (ii) the employment in other power electronics applications, possibly employing different neural networks.

REFERENCES

[1] P. Cortés, G. Ortiz, J. I. Yuz, J. Rodríguez, S. Vazquez, and L. G. Franquelo, "Model predictive control of an inverter with output *LC* filter for UPS applications," *IEEE Trans. Ind. Electron.*, vol. 56, no. 6, pp. 1875–1883, Jun. 2009.

[2] T. G. Habetler, R. Naik, and T. A. Nondahl, "Design and implementation of an inverter output *LC* filter used for dv/dt reduction," *IEEE Trans. Power Electron.*, vol. 17, no. 3, pp. 327–331, May 2002.

[3] M. P. Kazmierkowski and L. Malesani, "Current control techniques for three-phase voltage-source PWM converters: A survey," *IEEE Trans. Ind. Electron.*, vol. 45, no. 5, pp. 691–703, Oct. 1998.

[4] J. M. Carrasco, L. G. Franquelo, J. T. Bialasiewicz, E. Galván, R. C. P. Guisado, M. M. M. Prats, J. I. León, and N. Moreno-Alfonso, "Power-electronic systems for the grid integration of renewable energy sources: A survey," *IEEE Trans. Ind. Electron.*, vol. 53, no. 4, pp. 1002–1016, Jun. 2006.

[5] F. Blaabjerg, R. Teodorescu, M. Liserre, and A. V. Timbus, "Overview of control and grid synchronization for distributed power generation systems," *IEEE Trans. Ind. Electron.*, vol. 53, no. 5, pp. 1398–1409, Oct. 2006.

[6] J. M. Guerrero, L. G. De Vicuna, and J. Uceda, "Uninterruptible power supply systems provide protection," *IEEE Ind. Electron. Mag.*, vol. 1, no. 1, pp. 28–38, Feb. 2007.

[7] J. Y. Hung, W. Gao, and J. C. Hung, "Variable structure control: A survey," *IEEE Trans. Ind. Electron.*, vol. 40, no. 1, pp. 2–22, Feb. 1993.

[8] I. S. Mohamed, S. A. Zaid, M. F. Abu-Elyazeed, and H. M. Elsayed, "Classical methods and model predictive control of three-phase inverter with output *LC* filter for UPS applications," in *Proc. Int. Conf. Control, Decis. Inf. Technol. (CoDIT)*, May 2013, pp. 483–488.

[9] D. M. Brod and D. W. Novotny, "Current control of VSI-PWM inverters," *IEEE Trans. Ind. Appl.*, vol. IA-21, no. 3, pp. 562–570, May 1985.

[10] J. W. Jung, M. Dai, and A. Keyhani, "Optimal control of three-phase PWM inverter for UPS systems," in *Proc. IEEE Power Electron. Spec. Conf.*, vol. 3, Jun. 2004, pp. 2054–2059.

[11] I. S. Mohamed, S. A. Zaid, M. Abu-Elyazeed, and H. M. Elsayed, "Model predictive control-a simple and powerful method to control UPS inverter applications with output *LC* filter," in *Proc. Saudi Int. Electron., Commun. Photon. Conf. (SIECPC)*, Apr. 2013, pp. 1–6.

[12] F. Rojas, R. Kennel, R. Cardenas, R. Repenning, J. C. Clare, and M. Diaz, "A new space-vector-modulation algorithm for a three-level four-leg NPC inverter," *IEEE Trans. Energy Convers.*, vol. 32, no. 1, pp. 23–35, Mar. 2017.

[13] P. C. Loh, M. J. Newman, D. N. Zmood, and D. G. Holmes, "A comparative analysis of multiloop voltage regulation strategies for single and three-phase UPS systems," *IEEE Trans. Power Electron.*, vol. 18, no. 5, pp. 1176–1185, Sep. 2003.

[14] P. C. Loh and D. G. Holmes, "Analysis of multiloop control strategies for *LC/CL/LCL*-filtered voltage-source and current-source inverters," *IEEE Trans. Ind. Appl.*, vol. 41, no. 2, pp. 644–654, Mar. 2005.

[15] Y. A.-R. I. Mohamed and E. F. El-Saadany, "An improved deadbeat current control scheme with a novel adaptive self-tuning load model for a three-phase PWM voltage-source inverter," *IEEE Trans. Ind. Electron.*, vol. 54, no. 2, pp. 747–759, Apr. 2007.

[16] J. S. Lim, C. Park, J. Han, and Y. I. Lee, "Robust tracking control of a three-phase DC–AC inverter for UPS applications," *IEEE Trans. Ind. Electron.*, vol. 61, no. 8, pp. 4142–4151, Aug. 2014.

[17] M. Pichan, H. Rastegar, and M. Monfared, "Deadbeat control of the stand-alone four-leg inverter considering the effect of the neutral line inductor," *IEEE Trans. Ind. Electron.*, vol. 64, no. 4, pp. 2592–2601, Apr. 2017.

[18] G. Escobar, P. Mattavelli, A. M. Stankovic, A. A. Valdez, and J. Leyva-Ramos, "An adaptive control for UPS to compensate unbalance and harmonic distortion using a combined capacitor/load current sensing," *IEEE Trans. Ind. Electron.*, vol. 54, no. 2, pp. 839–847, Apr. 2007.

[19] S. Jiang, D. Cao, Y. Li, J. Liu, and F. Z. Peng, "Low-THD, fast-transient, and cost-effective synchronous-frame repetitive controller for three-phase UPS inverters," *IEEE Trans. Power Electron.*, vol. 27, no. 6, pp. 2994–3005, Jun. 2012.

[20] E. Wu and P. W. Lehn, "Digital current control of a voltage source converter with active damping of *LCL* resonance," in *Proc. 20th Annu. IEEE Appl. Power Electron. Conf. Expo. (APEC)*, vol. 3, Mar. 2005, pp. 1642–1649.

[21] H. Komurcugil, "Rotating-sliding-line-based sliding-mode control for single-phase UPS inverters," *IEEE Trans. Ind. Electron.*, vol. 59, no. 10, pp. 3719–3726, Oct. 2012.

[22] S. Sabir, Q. Khan, M. Saleem, and A. Khaliq, "Robust voltage tracking control of three phase inverter with an output *LC* filter: A sliding mode approach," in *Proc. 13th Int. Conf. Emerg. Technol. (ICET)*, Dec. 2017, pp. 1–5.

[23] P. Cortés, M. P. Kazmierkowski, R. Kennel, D. E. Quevedo, and J. R. Rodriguez, "Predictive control in power electronics and drives," *IEEE Trans. Ind. Electron.*, vol. 55, no. 12, pp. 4312–4324, Dec. 2008.

[24] V. K. Singh, R. N. Tripathi, and T. Hanamoto, "HIL co-simulation of finite set-model predictive control using FPGA for a three-phase VSI system," *Energies*, vol. 11, no. 4, p. 909, 2018.

[25] G. Willmann, D. F. Coutinho, L. F. A. Pereira, and F. B. Libano, "Multiple-loop H-infinity control design for uninterruptible power supplies," *IEEE Trans. Ind. Electron.*, vol. 54, no. 3, pp. 1591–1602, Jun. 2007.

[26] T. S. Lee, K. S. Tzeng, and M. S. Chong, "Robust controller design for a single-phase UPS inverter using μ-synthesis," *IEE Proc.-Electr. Power Appl.*, vol. 151, no. 3, pp. 334–340, 2004.

[27] M. Nauman and A. Hasan, "Efficient implicit model-predictive control of a three-phase inverter with an output *LC* filter," *IEEE Trans. Power Electron.*, vol. 31, no. 9, pp. 6075–6078, Sep. 2016.

[28] I. S. Mohamed, S. A. Zaid, M. F. Abu-Elyazeed, and H. M. Elsayed, "Implementation of model predictive control for three-phase inverter with output LC filter on eZdsp F28335 kit using HIL simulation," *Int. J. Model., Identificat. Control*, vol. 25, no. 4, pp. 301–312, 2016.

[29] L. Guo, N. Jin, C. Gan, L. Xu, and Q. Wang, "An improved model predictive control strategy to reduce common-mode voltage for two-level voltage source inverters considering dead-time effects," *IEEE Trans. Ind. Electron.*, vol. 66, no. 5, pp. 3561–3572, May 2019.

[30] E. F. Camacho and C. Bordons, "Nonlinear model predictive control: An introductory review," in *Assessment and Future Directions of Nonlinear Model Predictive Control*. Berlin, Germany: Springer, 2007, pp. 1–16.

[31] S. Vazquez, J. Rodriguez, M. Rivera, L. G. Franquelo, and M. Norambuena, "Model predictive control for power converters and drives: Advances and trends," *IEEE Trans. Ind. Electron.*, vol. 64, no. 2, pp. 935–947, Feb. 2017.

[32] H. T. Nguyen, E.-K. Kim, I.-P. Kim, H. H. Choi, and J.-W. Jung, "Model predictive control with modulated optimal vector for a three-phase inverter with an *LC* filter," *IEEE Trans. Power Electron.*, vol. 33, no. 3, pp. 2690–2703, Mar. 2017.

[33] S. Vazquez, A. Marquez, J. I. Leon, L. G. Franquelo, and T. Geyer, "FCS-MPC and observer design for a VSI with output *LC* filter and sinusoidal output currents," in *Proc. 11th IEEE Int. Conf. Compat., Power Electron. Power Eng. (CPE-POWERENG)*, Apr. 2017, pp. 677–682.

[34] I. S. Mohamed, S. A. Zaid, M. F. Abu-Elyazeed, and H. Elsayed, "Improved model predictive control for three-phase inverter with output *LC* filter," *Int. J. Model. Identificat. Control*, vol. 23, no. 4, pp. 371–379, 2015.

[35] T. Dragičević, "Model predictive control of power converters for robust and fast operation of AC microgrids," *IEEE Trans. Power Electron.*, vol. 33, no. 7, pp. 6304–6317, Jul. 2017.

[36] C. Zheng, T. Dragicevic, and F. Blaabjerg, "Current-sensorless finite-set model predictive control for *LC*-filtered voltage source inverters," *IEEE Trans. Power Electron.*, to be published.

[37] S. Mariéthoz and M. Morari, "Explicit model-predictive control of a PWM inverter with an *LCL* filter," *IEEE Trans. Ind. Electron.*, vol. 56, no. 2, pp. 389–399, Feb. 2009.

[38] S. Kwak and J.-C. Park, "Switching strategy based on model predictive control of VSI to obtain high efficiency and balanced loss distribution," *IEEE Trans. Power Electron.*, vol. 29, no. 9, pp. 4551–4567, Sep. 2014.

[39] M. H. Rashid, *Power Electronics Handbook*. Oxford, U.K.: Butterworth-Heinemann, 2017.

[40] K. S. Narendra and K. Parthasarathy, "Identification and control of dynamical systems using neural networks," *IEEE Trans. Neural Netw.*, vol. 1, no. 1, pp. 4–27, Mar. 1990.

[41] K. J. Hunt, D. Sbarbaro, R. Żbikowski, and P. J. Gawthrop, "Neural networks for control systems—A survey," *Automatica*, vol. 28, no. 6, pp. 1083–1112, 1992.

[42] J. Saint-Donat, N. Bhat, and T. J. McAvoy, "Neural net based model predictive control," *Int. J. Control*, vol. 54, no. 6, pp. 1453–1468, 1991.

[43] B. Karanayil and M. F. Rahman, "Artificial neural network applications in power electronics and electric drives," in *Power Electronics Handbook*, 4th ed. Amsterdam, The Netherlands: Elsevier, 2018, pp. 1245–1260.

[44] M. T. Wishart and R. G. Harley, "Identification and control of induction machines using artificial neural networks," *IEEE Trans. Ind. Appl.*, vol. 31, no. 3, pp. 612–619, May 1995.

[45] X. Sun, L. Chen, Z. Yang, and H. Zhu, "Speed-sensorless vector control of a bearingless induction motor with artificial neural network inverse speed observer," *IEEE/ASME Trans. Mechatronics*, vol. 18, no. 4, pp. 1357–1366, Aug. 2013.

[46] H.-Y. Lee, J.-L. Lee, S.-O. Kwon, and S.-W. Lee, "Performance estimation of induction motor using artificial neural network," in *Proc. 25th Int. Conf. Syst., Signals Image Process. (IWSSIP)*, Jun. 2018, pp. 1–3.

[47] S. M. Gadoue, D. Giaouris, and J. W. Finch, "Stator current model reference adaptive systems speed estimator for regenerating-mode low-speed operation of sensorless induction motor drives," *IET Electr. Power Appl.*, vol. 7, no. 7, pp. 597–606, 2013.

[48] A. Bakhshai, J. Espinoza, G. Joos, and H. Jin, "A combined artificial neural network and DSP approach to the implementation of space vector modulation techniques," in *Proc. IEEE Ind. Appl. Conf. 31st IAS Annu. Meeting*, vol. 2, Oct. 1996, pp. 934–940.

[49] J. O. P. Pinto, B. K. Bose, L. E. B. D. Silva, and M. P. Kazmierkowski, "A neural-network-based space-vector PWM controller for voltage-fed inverter induction motor drive," *IEEE Trans. Ind. Appl.*, vol. 36, no. 6, pp. 1628–1636, Nov. 2000.

[50] E. Karatepe and T. Hiyama, "Artificial neural network-polar coordinated fuzzy controller based maximum power point tracking control under partially shaded conditions," *IET Renew. Power Gener.*, vol. 3, no. 2, pp. 239–253, 2009.

[51] M. P. Akter, S. Mekhilef, N. M. L. Tan, and H. Akagi, "Modified model predictive control of a bidirectional AC–DC converter based on Lyapunov function for energy storage systems," *IEEE Trans. Ind. Electron.*, vol. 63, no. 2, pp. 704–715, Feb. 2016.

[52] B.-R. Lin and R. G. Hoft, "Power electronics inverter control with neural networks," in *Proc. 8th Annu. Appl. Power Electron. Conf. Expo.*, Mar. 1993, pp. 128–134.

[53] X. Sun, M. H. L. Chow, F. H. F. Leung, D. Xu, Y. Wang, and Y.-S. Lee, "Analogue implementation of a neural network controller for UPS inverter applications," *IEEE Trans. Power Electron.*, vol. 17, no. 3, pp. 305–313, May 2002.

[54] H. Boumaaraf, A. Talha, and O. Bouhali, "A three-phase NPC grid-connected inverter for photovoltaic applications using neural network MPPT," *Renew. Sustain. Energy Rev.*, vol. 49, pp. 1171–1179, Sep. 2015.

[55] R. J. Wai, M. W. Chen, and Y. K. Liu, "Design of adaptive control and fuzzy neural network control for single-stage boost inverter," *IEEE Trans. Ind. Electron.*, vol. 62, no. 9, pp. 5434–5445, Sep. 2015.

[56] X. Fu and S. Li, "Control of single-phase grid-connected converters with *LCL* filters using recurrent neural network and conventional control methods," *IEEE Trans. Power Electron.*, vol. 31, no. 7, pp. 5354–5364, Jul. 2016.

[57] I. S. Mohamed, S. A. Zaid, H. M. Elsayed, and M. F. Abu-Elyazeed, "Three-phase inverter with output *LC* filter using predictive control for UPS applications," in *Proc. Int. Conf. Control, Decis. Inf. Technol. (CoDIT)*, May 2013, pp. 489–494.

[58] S. Piche, B. Sayyar-Rodsari, D. Johnson, and M. Gerules, "Nonlinear model predictive control using neural networks," *IEEE Control Syst.*, vol. 20, no. 3, pp. 53–62, Jun. 2000.

[59] B. M. Åkesson and H. T. Toivonen, "A neural network model predictive controller," *J. Process Control*, vol. 16, no. 9, pp. 937–946, 2006.

[60] D. Wang, X. Yin, S. Tang, C. Zhang, Z. J. Shen, J. Wang, and Z. Shuai, "A deep neural network based predictive control strategy for high frequency multilevel converters," in *Proc. IEEE Energy Convers. Congr. Expo. (ECCE)*, Sep. 2018, pp. 2988–2992.

[61] T. Dragičević and M. Novak, "Weighting factor design in model predictive control of power electronic converters: An artificial neural network approach," *IEEE Trans. Ind. Electron.*, vol. 66, no. 1, pp. 8870–8880, Nov. 2018.

[62] K. Hornik, "Approximation capabilities of multilayer feedforward networks," *Neural Netw.*, vol. 4, no. 2, pp. 251–257, 1991.

[63] NVIDIA. (Jun. 2019). *Training With Mixed Precision*. [Online]. Available: https://docs.nvidia.com/deeplearning/sdk/pdf/Training-Mixed-Precision-User-Guide.pdf

[64] D. Das, N. Mellempudi, D. Mudigere, D. Kalamkar, S. Avancha, K. Banerjee, S. Sridharan, K. Vaidyanathan, B. Kaul, E. Georganas, A. Heinecke, P. Dubey, J. Corbal, N. Shustrov, R. Dubtsov, E. Fomenko, and V. Pirogov, "Mixed precision training of convolutional neural networks using integer operations," 2018, *arXiv:1802.00930*. [Online]. Available: https://arxiv.org/abs/1802.00930

[65] Z. Hu, A. B. Tarakji, V. Raheja, C. Phillips, T. Wang, and I. Mohomed, "Deepome: Distributed inference with heterogeneous devices in the edge," in *Proc. 3rd Int. Workshop Deep Learn. Mobile Syst. Appl. (EMDL)*, New York, NY, USA, 2019, pp. 13–18.

[66] M. F. Møller, "A scaled conjugate gradient algorithm for fast supervised learning," *Neural Netw.*, vol. 6, no. 4, pp. 525–533, Nov. 1993.

[67] R. Fletcher, *Practical Methods of Optimization*, 2nd ed. Hoboken, NJ, USA: Wiley, 2000.

IHAB S. MOHAMED received the B.S. degree from the Institute of Aviation Engineering and Technology (IAET), Egypt, in 2009, the M.S. degree in electrical engineering from Cairo University, Egypt, in 2014, and the M.Sc. degree in European master in advanced robotics (EMARO+). He attended the first year of EMARO+ at the Warsaw University of Technology (WUT), Poland, and the second year at the University of Genoa (GU), Italy. He is currently pursuing the Ph.D. degree in robotics engineering with INRIA Sophia Antipolis—Méditerranée, Université Côte d'Azur, France, under the supervision of Prof. P. Martinet, G. Allibert, and P. Salaris.

From 2009 to 2015, he was a Teaching Assistant with the Electronics and Communications Department, IAET. His research interests include predictive control (MPC), power electronics, robotics, computer vision, and machine learning.

STEFANO ROVETTA (M'99–SM'12) is currently an Associate Professor of computer science with the University of Genova, Italy. He has authored more than 170 scientific articles in machine learning, neural networks, clustering, fuzzy systems, and bioinformatics.

Dr. Rovetta is a member of the Italian Neural Network Society, the European Neural Network Society, and the European Society for Fuzzy Logic and Technology. He received the 2008 Pattern Recognition Society Award. He was the Chair of international conferences.

TON DUC DO (S'12–M'14) received the B.S. and M.S. degrees from the Hanoi University of Science and Technology, Hanoi, Vietnam, in 2007 and 2009, respectively, and the Ph.D. degree from Dongguk University, Seoul, South Korea, in 2014, all in electrical engineering.

From 2008 to 2009, he was a Lecturer with the Division of Electrical Engineering, Thuy Loi University, Vietnam. He was a Postdoctoral Researcher with the Division of Electronics and Electrical Engineering, Dongguk University, in 2014. He was also a Senior Researcher with the Pioneer Research Center for Controlling Dementia by Converging Technology, Gyeongsang National University, South Korea, from May 2014 to August 2015. Since September 2015, he has been an Assistant Professor with the Department of Robotics and Mechatronics, Nazarbayev University, Kazakhstan. His research interests include advanced control system theories, electric machine drives, renewable energy conversion systems, uninterruptible power supplies, electromagnetic actuator systems, targeted drug delivery systems, and nanorobots.

Dr. Do received the Best Research Award from Dongguk University, in 2014. He was a Lead Guest Editor for the special issue of Mathematical Problems in Engineering on *Advanced Control Methods for Systems with Fast-Varying Disturbances and Applications*. He is currently an Associate Editor of IEEE Access.

TOMISLAV DRAGIČEVIĆ (S'09–M'13–SM'17) received the M.Sc. and Industrial Ph.D. degrees in electrical engineering from the Faculty of Electrical Engineering, Zagreb, Croatia, in 2009 and 2013, respectively.

From 2013 to 2016, he was a Postdoctoral Research Associate, and since March 2016, he has been an Associate Professor with Aalborg University, Denmark, where he leads the Advanced Control Lab. He made a guest professor stay at Nottingham University, U.K., in 2018. He has authored or coauthored more than 170 technical articles (more than 70 of them are published in international journals, mostly IEEE Transactions) in his domain of interest, eight book chapters, and a book in the field. His research interests include design and control of microgrids, and application of advanced modeling and control concepts to power electronic systems.

Dr. Dragičević was a recipient of the Končar Prize for the best industrial Ph.D. thesis in Croatia, and the Robert Mayer Energy Conservation Award. He serves as an Associate Editor for the IEEE Transactions on Industrial Electronics, the IEEE Journal of Emerging and Selected Topics in Power Electronics, and the *IEEE Industrial Electronics Magazine*.

AHMED A. ZAKI DIAB received the B.Sc. and M.Sc. degrees in electrical engineering from Minia University, Egypt, in 2006 and 2009, respectively, and the Ph.D. degree from the Electric Drives and Industry Automation Department, Faculty of Mechatronics and Automation, Novosibirsk State Technical University, Novosibirsk, Russia, in 2015. Since 2001, he has been with the Department of Electrical Engineering, Faculty of Engineering, Minia University, as a Teaching Assistant, a Lecturer Assistant, and since 2015, as an Assistant Professor. His current research interests include ac drives, application of control techniques, and optimization algorithms in renewable energy systems. He was a recipient of the Postdoctoral Fellowship at the National Research University, Moscow Power Engineering Institute (MPEI), Moscow, Russia, from September 2017 to March 2018.

• • •